Seismic monitoring in Greece, 1899–2014: catalogue completeness 1966–2014

N. S. Melis [1], K. Lentas [1] and D. Schorlemmer[2]

[1]*Institute of Geodynamics, National Observatory of Athens, Lofos Nymfon, Thissio,* 11810 *Athens, Greece. E-mail:* nmelis@noa.gr
[2]*GFZ German Research Centre for Geosciences, Telegrafenberg,* 14473 *Potsdam, Germany*

SUMMARY

Instrumental earthquake monitoring in Greece started in 1899–1906 with the first five seismic stations of the National Observatory of Athens, Institute of Geodynamics (NOA). Subsequent upgrades and expansions led to today's Unified National Seismic Network, which includes almost all permanent seismic stations in Greece and provides waveform and parametric data. We examine the detection capabilities of the Greek seismic networks using phase, location and magnitude data from the International Seismological Centre (ISC) and the various National Institutes. We apply two methods to measure the network performance. In one, we form a grid, and find the 50 per cent probability detection threshold for each station-grid cell pair for different times. In the other, we find the probability-based magnitude of completeness grid for every three months from 1970 to 2014. Both methods show that in 1990 the detection threshold improved significantly in the north part of Greece. A much greater improvement took place in 2010 throughout Greece, yielding a completeness magnitude of $M_p \sim 1$.

Key words: Spatial analysis; Body waves; Earthquake hazards; Seismic instruments; Statistical seismology.

1 INTRODUCTION

Seismic networks observe earthquakes and produce seismic catalogues, which are used for earthquake hazard and seismicity-rate studies (e.g. Toda 2002; Lombardi *et al*. 2010; Li *et al*. 2020). Their usefulness increases with their completeness, which is quantified primarily by the completeness magnitude (M_c). Classically, the completeness magnitude is calculated directly from seismic catalogues as the deviation from the assumed log-linear frequency–magnitude distribution (*b*-value) based on the Gutenberg–Richter relation (e.g. Wiemer & Wyss 2000; Woessner & Wiemer 2005). Such a calculation always requires a set of earthquakes (preferably 200 or more) which are spread over a spatio-temporal volume, and sometimes may include local or temporal variations of the detection capabilities. Neglecting these spatio-temporal variations of completeness may lead to erroneous determinations of seismicity rates. By the term spatio-temporal variations we refer to a number of different factors, namely, the history of the network, processing methods and data analysis (Yamada *et al*. 2011; Kuyuk & Allen 2013; Landro *et al*. 2019; Lentas & Harris 2019).

In this paper, we focus on the permanent seismic networks operating in Greece since the beginning of the instrumental era (1903). Greece is located on a tectonically active plate boundary where the oceanic African lithospheric plate is subducting beneath the continental Eurasian plate in a highly varied rate along strike. The southern portion of the Hellenic subduction zone shows reverse faulting

seismicity that varies in depth from the surface to depths of ~200–300 km, while the northern part is associated with normal faulting and strike-slip crustal earthquakes mainly (Ambraseys & Jackson 1990; Papazachos 1990; Nyst & Thatcher 2004; Leptokaropoulos *et al*. 2012; Saltogianni *et al*. 2020).

Only a few attempts were carried out in the past to evaluate the performance and completeness magnitude of these networks through time. For example, D'Alessandro *et al*. (2011) studied a limited time period (three years) of the Hellenic Unified Seismological Network (HUSN, from 2007 to 2010 June), in order to evaluate the location performance of the network by numerical simulation as a function of magnitude and hypocentral depth. Mignan & Chouliaras (2014) determined the completeness magnitude of the network operated by the National Observatory of Athens (NOA) from 1964 to 2013, using the seismic catalogue of NOA only, which may have neglected the availability of small-magnitude earthquakes detected and reported by the network of the Aristotle University of Thessaloniki (THE) in Northern Greece. More importantly, both of these studies neglected the use of additional spatio-temporal information, such as the picked phase arrivals which are associated with the seismic events in the catalogues and which can provide more realistic estimation of the temporal capabilities of the network.

In this study, we assess the seismic event detection capability and completeness magnitude of the permanent networks operating in Greece throughout the entire period of their operation, by taking into account every available seismic event in any existing catalogue
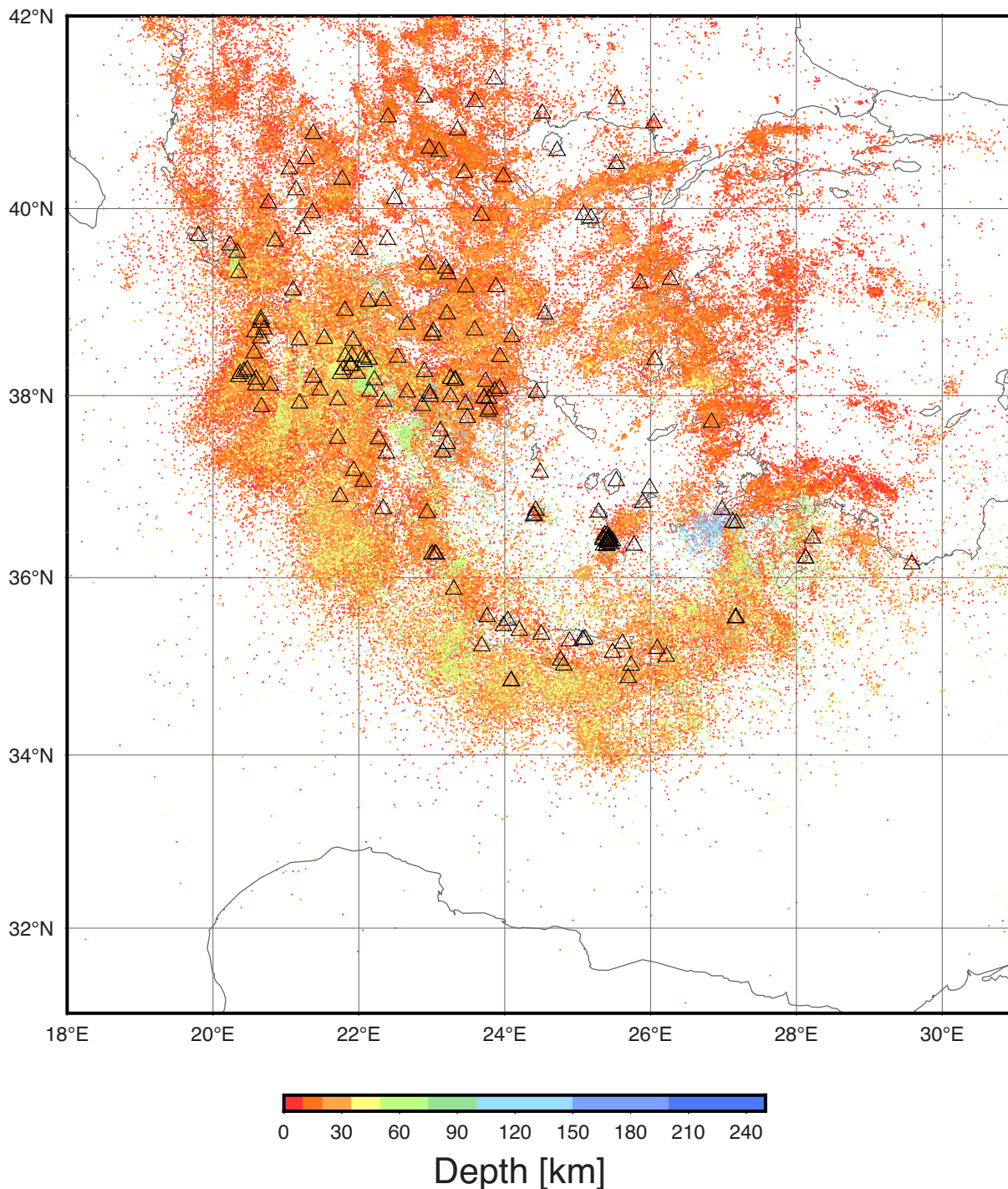
Figure 1. Spatial distribution of the seismicity used in the current study (International Seismological Centre 2022) as dots, colour-coded by depth and the locations of the stations (triangles) of the HUSN.

in the area. To do so, we use manually picked phase arrivals and we apply two different techniques, namely, we calculate station detection capability thresholds (e.g. Kvaerna & Ringdal 2013), and we carry out a probabilistic magnitude of completeness (PMC) assessment (Schorlemmer & Woessner 2008) which provides a full description of the detection probabilities over space, time and magnitude.

2 DATA

The region under investigation spans the area from from 18°E to 31°E in longitude and 31°N to 42°N in latitude. We used parametric earthquake data from a total of 177 stations. These stations were initially installed by NOA, while further stations operated by other research institutes in Greece were later incorporated into the HUSN (see Fig. 1, and Table S1 and Fig. S1 in the Supporting Information).
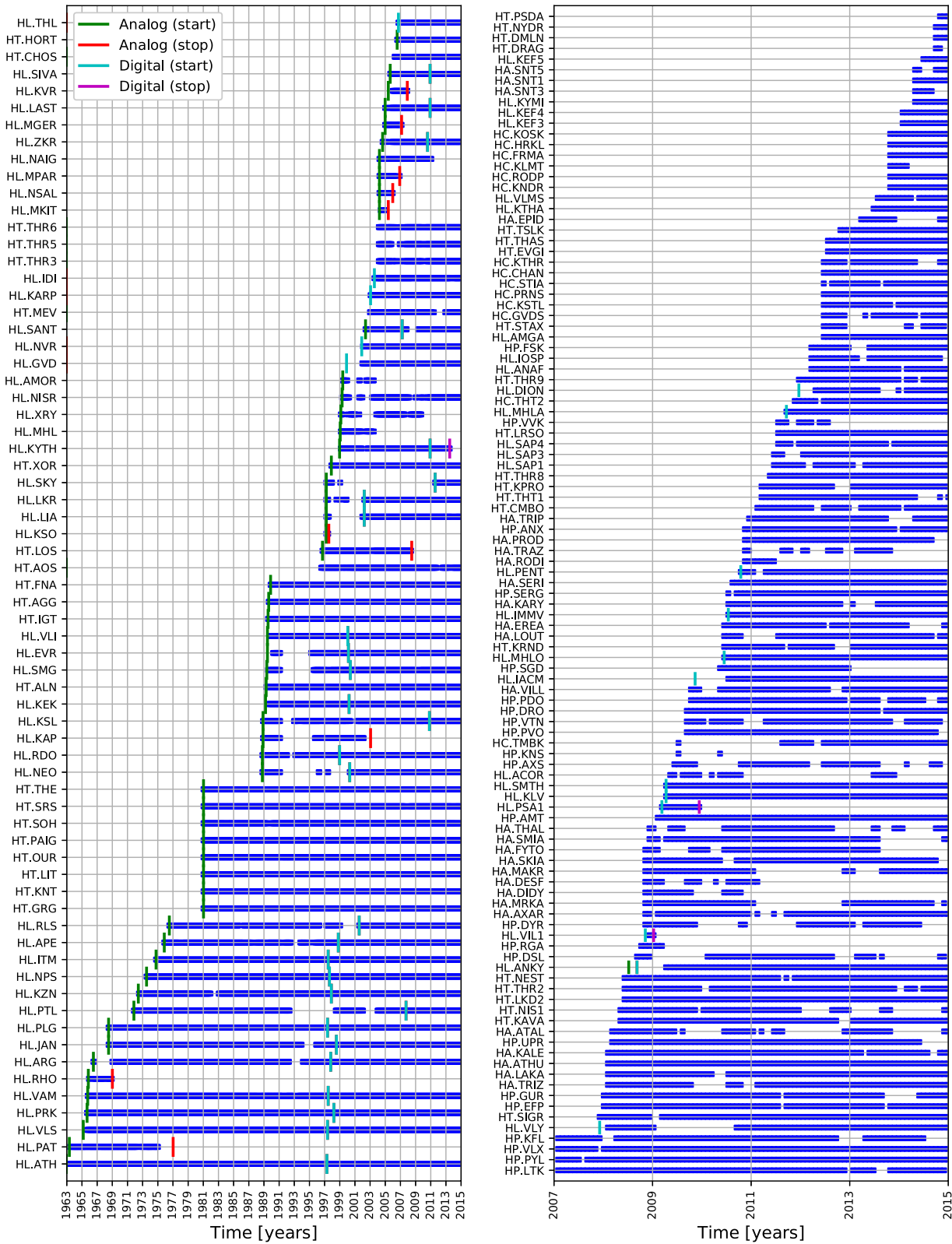
Figure 2. Time coverage of phase picks for the seismic stations operated in Greece since 1963. Stations (network code and station code) are shown on the vertical axis and time (in years) is shown on the horizontal axis. The left frame shows stations that have been converted from analogue to digital operation, whilst the right frame shows digital stations only. Green and red markers show start and stop times for the analogue operation, whereas cyan and magenta markers indicate these for the digital operation. Markers are shown only for the cases where precise information is available. Large gaps in the plots are indicative of malfunctions in the instruments or telemetry. Note the difference in the timescale between the left and right frames. Small gaps may be hidden in the left frame.
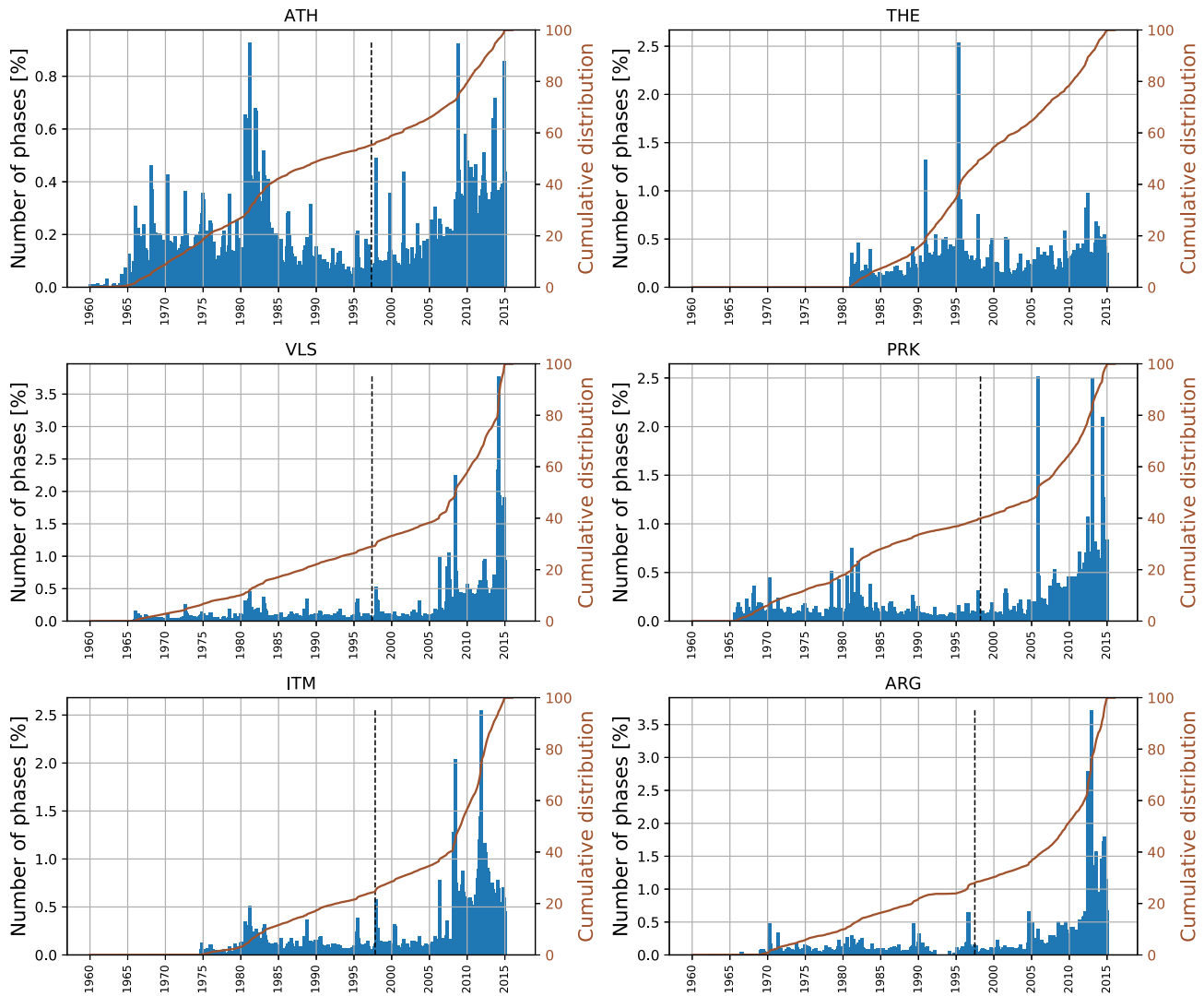
Figure 3. Histograms showing the percentage of picked phases over time for the stations ATH (Athens), THE (Thessaloniki), VLS (Valsamata), PRK (Ag. Paraskevi), ITM (Ithomi) and ARG (Archangelos). The brown lines show the cumulative distributions, and the black dashed lines indicate the times when a station was converted from analogue to digital operation.

They are considered to be permanent installations, and despite periods of disruption they report continuously most of the time. Fig. 2 shows the distribution of seismic-phase reporting over time for the stations in the current study. In a few cases, stations experienced technical problems during the first days of operation (i.e. ARG, DION, IACM and VLY) or they never worked properly until they were upgraded to digital operation (i.e. LIA and ANKY).

We extracted all reported phase arrivals from the Bulletin of the International Seismological Centre (ISC, International Seismological Centre 2022) for each station. This covers the period from 1905 November, when the first seismic station (Athens, ATH) in Greece was installed and taken into operation, to the most recent reviewed month (2014 December) added to the ISC reviewed bulletin (ISC database last accessed in 2017 December, International Seismological Centre 2022, see e.g. Fig. 3). The ISC collects bulletins from many available sources, and for Greece, bulletins from both the NOA and the THE are merged together into a single bulletin. Several peaks of activity can be identified in Fig. 3, with the most prominent in 1981 for the ATH station which is associated with the

1981 February 24, M_L^{NOA} 6.3, Alkyonides (Gulf of Corinth) earthquake, and the 1995 May 13, M_L^{NOA} 6.1, Kozani–Grevena (North Greece) earthquake at the THE (Thessaloniki) station, respectively. Even though the network operation was planned to be switched to digital in 1997, a substantial increase in the reported phase arrivals can only be observed from 2007 onwards, since improvements in telecommunications started in 2000 and during 2003–2004 the first Seedlink server came into operation. The latter made an improvement in accessing waveform data, minimizing data gaps, ensuring automatic operational procedures and implementing quality controls of the whole network. It is worth noting that we had to make some minor corrections: we merged phase arrivals from 1965 to 1979 of the station RHD (Rhodes) with those of the station ARG (Arkhangelos). Both station codes represent essentially the same station at the same vault. This merge was resolved through careful inspection of the NOA Bulletin hard copy at the NOA library. In addition, the station KAP (Karpathos) operated from 1988 to 2003 and was moved to a new site and vault (KARP). Thus, a few picks from 2003 that were initially reported from station KAP needed to be associated with station KARP.

We used the prime hypocentre solutions in the ISC Bulletin, which includes both unreviewed and reviewed events. A subset of reviewed events is also relocated by the ISC if certain criteria are met (see e.g. the Summary of the Bulletin of the International Seismological Centre, International Seismological Centre 2013). Because the main seismicity in Greece occurs along the Hellenic trench, and the majority of the stations are located northwards and eastwards of the trench providing a relatively narrow azimuthal coverage for the NOA stations, it is expected that NOA locations will suffer from biases introduced by correlated theoretical traveltime errors due to the unmodelled 3-D Earth's structure. By using ISC locations for these events, where additional station phase arrivals from neighbouring networks are also being used, it is expected to achieve more robust locations with narrower azimuthal gaps (Bondár & Storchak 2011). It is worth noting that while Melis & Konstantinou (2006) report the first automatic processing procedure for Greece, they noted that other stations from neighbouring networks, such as MEDNET (Mediterrean Network), GEOFON at GFZ (GeoForschungsZentrum Potsdam, Germany) and IRIS (Incorporated Research Institutions for Seismology, USA) were available in real-time and could be used to minimise the station azimuthal gap, hence, further strengthen the automated location procedure.

Moreover, we extracted all available magnitudes, regardless of the magnitude type, that were reported to ISC. This search resulted in 2 77 547 seismic events for the entire period within the area of interest. In order to compile the final data set, we considered only seismic events that have at least one associated magnitude estimation and were reported by at least three stations. Prior to 1964, M_S^{ISC} is the predominantly available magnitude type for the majority of events in our data set. From 1964 to 1971, m_b^{ISC} is the dominant magnitude type, whereas for the period covering 1971 to 1985, m_b^{ISC} and M_L^{NOA} are the main available magnitude types. From 1985 onwards, M_L^{NOA} and M_D^{NOA} are the main preferred magnitude types. It it worth mentioning that in many cases (up to 1985), usually small magnitude events (<4.0) have no magnitude type specified, nevertheless, they have been included in our data set, since it is important to be as complete as possible within the low magnitude range, and they cover only a small portion with respect to the entire data set. These constraints yielded 2 28 176 seismic events starting from 1963.

3 METHOD

In order to assess the performance of the seismic stations operating in Greece, we focus our analysis during the period from 1963 to 2014, since the data prior to this (1905–1963) is not adequate as the network was too sparse and many small earthquakes were most likely undetected. Specifically, we applied two different methods: (i) a method for the quantification of event detection capability thresholds at individual stations (Kvaerna & Ringdal 2013), and (ii) the PMC technique (Schorlemmer & Woessner 2008).

3.1 Station detection capability thresholds and sensitivity

The estimation of individual station detection-capability thresholds is based on the 'Method 1' as referred in Kvaerna & Ringdal (2013), which is based on the method developed by Ringdal (1975). Given a source area, the probability $P_i(M_j)$ of detecting an event j with magnitude M_j at a station i can be expressed as:

$$P_i(M_j) = \Phi\left(\frac{M_j - \mu_i}{\sigma_i}\right), \tag{1}$$

where Φ denotes the cumulative function of the distribution resulting from the number of detected phases by the station i with respect to the magnitudes M_j, which is expected to follow a normal distribution, μ_i represents the 50 per cent detection threshold and σ_i is the standard deviation of the detection curve at the ith station.

For a group of E seismic events, located within the source area of interest, and detected by the seismic station i under investigation, a likelihood function is defined as follows:

$$L(\mu, \sigma) = \prod_{k \in E} \Phi\left(\frac{M_k - \mu}{\sigma}\right) \prod_{k \notin E}\left[1 - \Phi\left(\frac{M_k - \mu}{\sigma}\right)\right]. \tag{2}$$

The 50 per cent detection threshold μ, is the one that maximizes eq. (2).

In our study, we split the area of interest in a regular grid of $0.2° \times 0.2°$ (Fig. 4) and, as stated in Section 2, we consider only seismic events that were reported by at least three stations. For each seismic station, we count the detected and non-detected events within each cell of the grid and we fit a cumulative Gaussian distribution curve to the observed cumulative distribution of detected events by means of least squares. The 50 per cent detection threshold for each station-grid cell pair is then estimated from the corresponding cumulative distribution curve (Fig. 5).

So far, we examined the detection capability of the network based on the assumption that each event should be reported by at least three stations. Nevertheless, source effects (source mechanism) and/or local effects (site conditions and background noise level) may have an impact on the event detection capabilities of single stations. Even though it is expected that the minimum magnitude of a seismic event detected on a single station decreases with distance, and vice versa, it is very rare that a clear distinction between detected and non-detected events is observed as a function of magnitude and distance. Therefore, when studying the detection capabilities of single stations it is necessary to correct for the hypocentral distance effect. Based on eq. (1), we calculated the probability $P_i(M_L, R)$, which is a corrected probability for the local magnitude (M_L) specifically, that takes into account the hypocentral distance R (Morandi & Matsumura 1991). The local magnitude is calculated using an attenuation curve based on Hutton & Boore (1987), for $R < 1000$ km:

$$M_L = \log_{10}(A) + 1.11 \log_{10}(R) + 0.00189R - 2.09, \tag{3}$$

where A is the amplitude of the signal in metres. Reworking eq. (3) as follows:

$$M_L - 1.11 \log_{10}(R) - 0.00189R = \log_{10}(A) - 2.09, \tag{4}$$

and introducing a reduced magnitude $M_L' = \log_{10}(A) - 2.09$, we get:

$$M_L' = M_L - 1.11 \log_{10}(R) - 0.00189R. \tag{5}$$

Finally, the probability $P_i(M_L, R)$ is defined in a similar manner as in eq. (1):

$$P_i(M_L, R) = \Phi\left(\frac{M_L' - \mu_i}{\sigma_i}\right). \tag{6}$$

The value of M_L' at 50 per cent probability (i.e. $M_L' = \mu_i$) is directly associated with the sensitivity of the station. Thus, small values of μ_i indicate stations of high sensitivity. On the contrary, the higher the value of μ_i is, the less sensitive the station is. Fig. 6 shows an example for the station Griva (GRG), which shows a higher sensitivity in the latter period of its operation (2007–2014), possibly as a result of its digitization, even though we could not confirm the exact date that this took place, hence, this is not mentioned in Fig. 2.
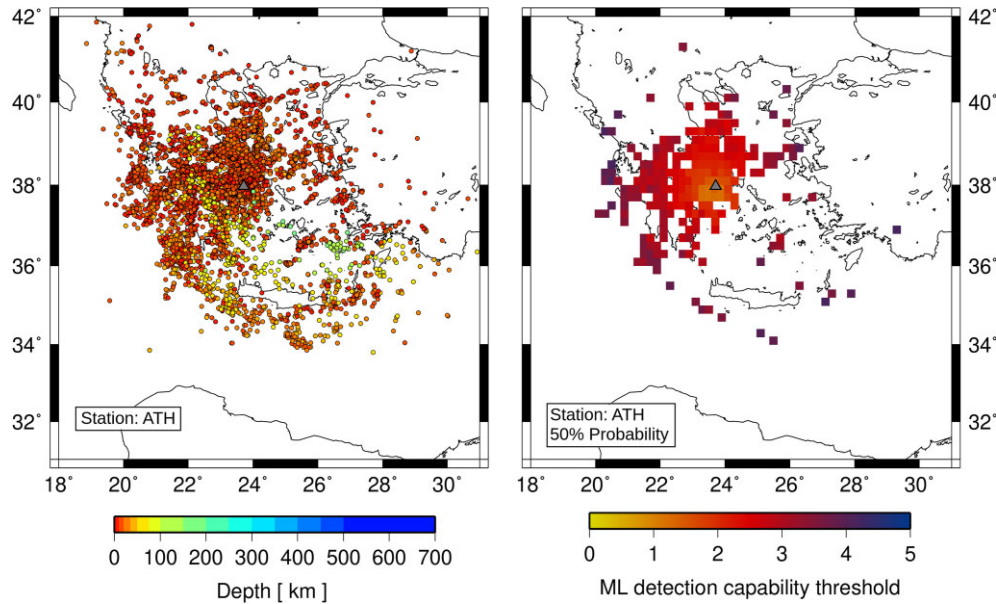
Figure 4. Map showing the seismicity (colour-coded by depth) associated with the picked phase arrivals at the ATH (Athens) station during the time period from 2007 to 2014 (left). Map showing the M_L detection-capability thresholds calculated for each grid cell using the technique described in Section 3.1 for the ATH station (right). The station is plotted on each map as a grey triangle.
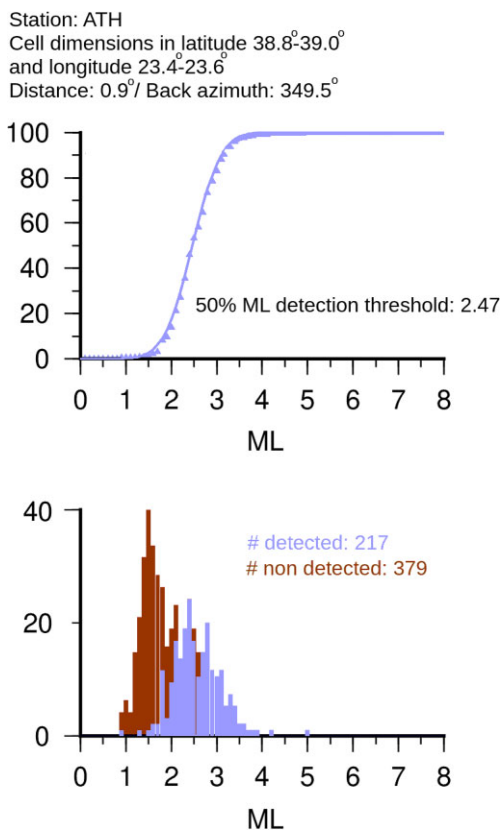

Figure 5. An illustrative example for the determination of the 50 per cent detection threshold at station ATH for the seismicity (2007–2014) within the grid cell located offshore North Evia island. The detection threshold is determined by fitting a Gaussian function (purple line) to the cumulative distribution (purple triangles) shown in the probability–magnitude plot in the top frame which is a result of the histogram of the detected events (purple bars) shown in the bottom frame. Brown bars represent the distribution of the non-detected events in the grid cell by the station. The number of the detected and non-detected events within the grid cell are shown in purple and brown in the bottom frame.

3.2 Probabilistic magnitude of completeness (PMC) method

In conjuction with the method above, we applied the PMC method developed by Schorlemmer & Woessner (2008). A detailed description of the method is given in the publication, and hence, we will only briefly discuss the main concepts of it.

The PMC method uses empirical data only, such as hypocentre locations, station phase arrivals, earthquake magnitudes, as well as the attenuation curve used for the magnitude determination. The method consists of two major parts, namely, the analysis and the synthesis. In the analysis part, the detection probabilities for each station $P_D(M, L)$ are calculated as a function of magnitude, M, and distance of the event from the station, L. These probabilities are estimated from the picked or missed phases at each particular station, taking into account the used magnitude attenuation model. These probabilities are assumed to be isotropic. In the synthesis part, they are used to compute the event-detection probabilities $P_E(M, \mathbf{x})$, where M is the magnitude of an event and $\mathbf{x}$ its location (longitude, and depth). This probability is defined as the joint probability that four (by default) or more stations have detected the event with magnitude M at location $\mathbf{x}$. In this study we have adjusted the triggering conditions to three stations as used by the network. From these probabilities P_E, the PMC, $M_P(\mathbf{x}, P)$, where P is the detection probability and $\mathbf{x}$ is the location, can be calculated. In the synthesis part, only stations that are in operation and used for triggering the location procedure should be considered. Likewise, in the analysis part, stations not in operation should not be penalized for missing earthquakes. Thus, the respective probabilities should be computed for periods in which the triggering conditions of the network and the magnitude definition are constant and clusters or aftershocks should be avoided, referred to as period of homogeneous recording. This ultimately makes P_E and M_P functions of time.

Unlike more traditional and simplistic techniques (e.g. Wiemer & Wyss 2000; Woessner & Wiemer 2005), PMC avoids most of the assumptions on the calculation of the completeness magnitude, for example, Gutenberg–Richter distribution.
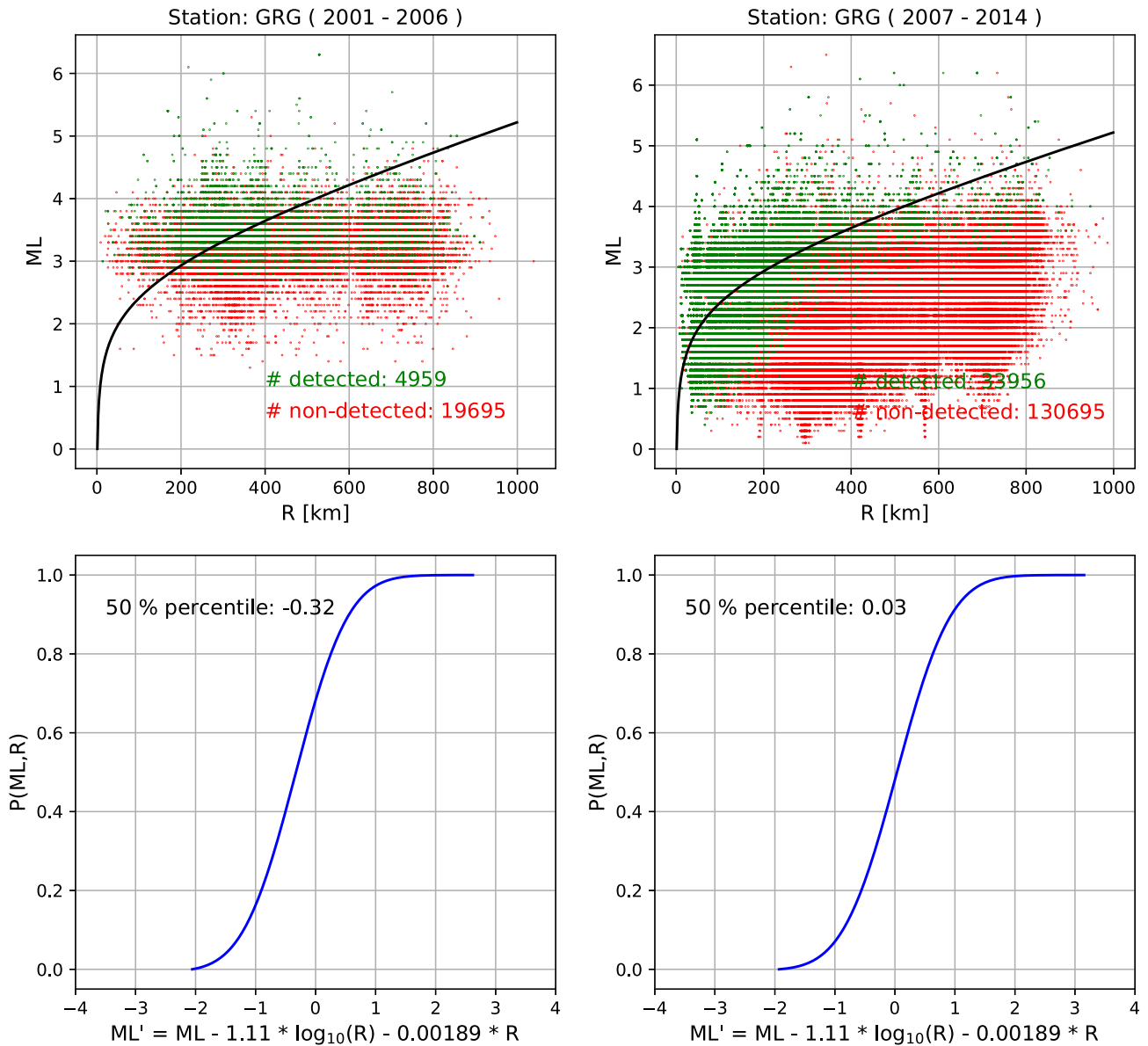
Figure 6. An example of reduced magnitude, M'_L, determination at station Griva (GRG) for the period from 2001 to 2006 (left) and the period from 2007 to 2014 (right). The top plots show the distribution of seismic events detected by the station (green dots) and not detected (red dots). The black line represents the attenuation curve of eq.(5) that corresponds to the reduced magnitude (M'_L). The cumulative distribution of the best-fitting Gaussian curve to the data is shown in blue (bottom).

In this study, both the analysis and synthesis was calculated for periods of three months. The on-/off-times of the stations were estimated directly from the phase-arrival picks and later used to estimate the set of operational stations per period.

4 RESULTS

4.1 Detection capability thresholds and sensitivity of the NOA stations

To calculate station detection thresholds, we split the data into four main periods. These are:

(i) The period from 1963 to 1980. During this period only NOA seismic stations were in operation.

(ii) The period from 1981 to 2000, when seismic stations installed by the THE in northern Greece.

(iii) The period from 2001 to 2006, when some stations were converted from analogue to digital operation.

(iv) The period from 2007 to 2014, when all the stations work as digital stations.

For the two first periods (1963–2000), we mainly use the M_L^{NOA} magnitude, and the m_b^{ISC} magnitude only for earthquakes within the area of interest which were not detected by NOA, meaning that they may be detected by some other agency in the area, or there is no M_L^{NOA} available. In the two remaining periods, we use either M_L^{NOA} or M_D^{NOA} magnitudes, assuming $M_L \sim M_D$ for $M_L > 3.0$ (Kiratzi & Papazachos 1984; Melis et al. 1989). Fig. S2 in the Supporting Information shows the frequency distribution of
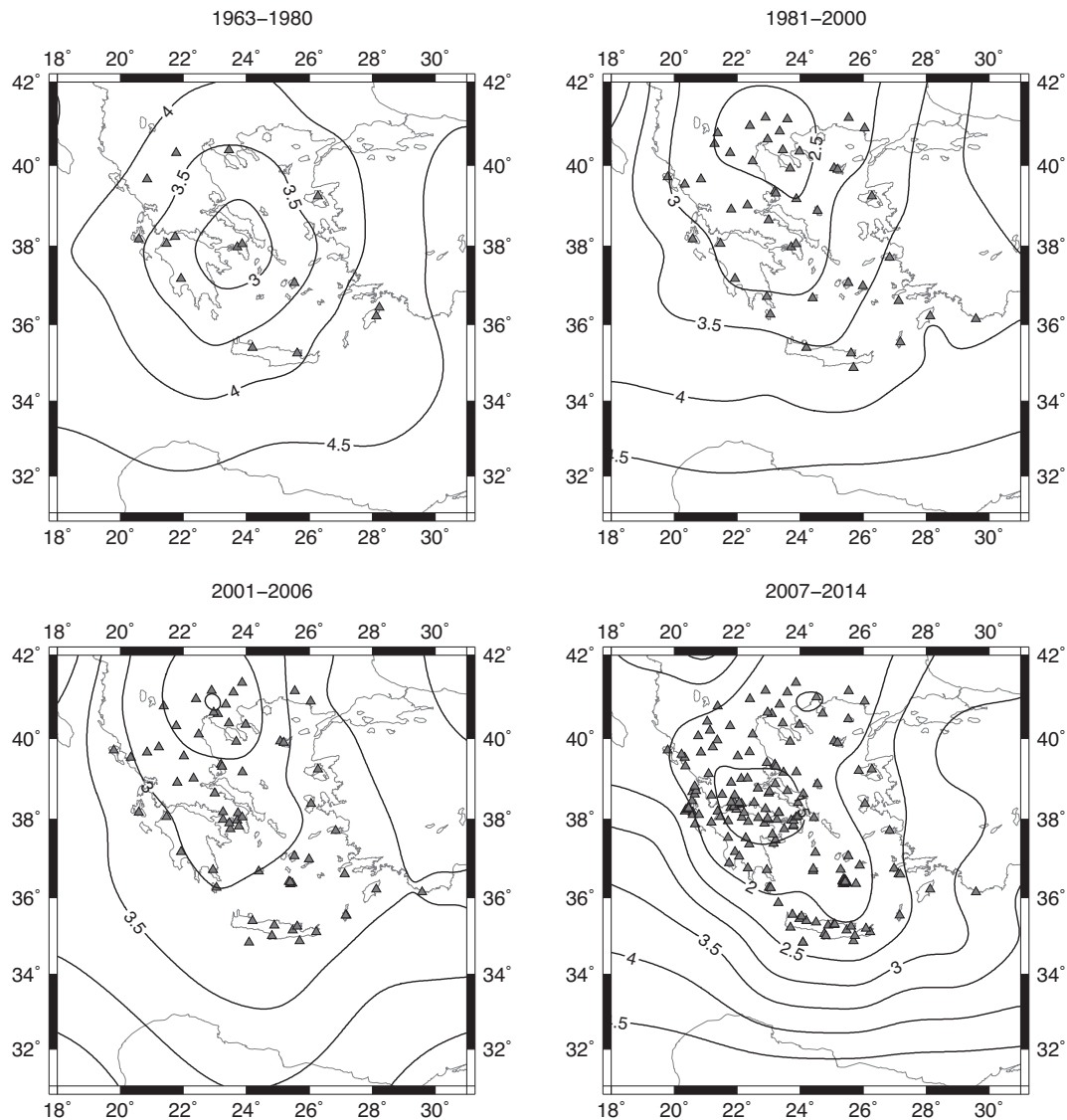
Figure 7. Maps showing the spatial distribution of 50 per cent detection capability thresholds bsed on the stations (grey triangles) operated in Greece over different periods. M_L magnitudes were specifically used for the period from 2001 to 2014, whereas, for earlier periods (1963–2000) the use of different magnitude types was inevitable.

available magnitude types in our data set over the examined time period.

After splitting the area of interest into a $0.2° \times 0.2°$ regular grid, and calculating the 50 per cent detection thresholds for each station-grid cell pair and each period as explained in Section 3.1, we grouped the results in four separate maps, each one representing one period (Fig. 7). The detection thresholds in this study represent the capability of the network to detect an earthquake recorded by at least three stations (see also eq. 2). It is obvious that the performance of the NOA network during the early period (1963–1980) is poorer compared to more modern years, and only earthquakes of magnitude $M \gtrsim 3$ were detected. The same applies for the second period (1981–2000), with northern Greece showing a minimum primarily due to the operation of the stations maintained by THE, focusing mainly on the local seismicity. During the third period (2001–2006) which marks the beginning of the digital era of the NOA network, there is a small improvement observed in southern Greece, namely the $M3.5$ contour is moved south of the coast of Crete island, as a result

of a few more stations installed on the island. A few more stations were installed in mainland Greece too, nevertheless, their contribution in terms of completeness is negligible. The most substantial change in the performance of the network is observed during the last period (2007–2014), when all stations of the so-called HUSN are being used by NOA. The detection thresholds of the stations have dropped dramatically during this period and the minimum detection thresholds appear in the centre of the network, as expected, due to the uniform distribution of the network's seismic stations.

Fig. 8 summarizes individual station sensitivity (μ) calculations for the different periods (see e.g. Fig. 6). During the first and second periods (1963–2000), the most sensitive stations ($\mu < 0$) appear to be those in southern Greece, where most of the seismicity is observed around the Hellenic trench. During the second period (1981–2000), stations in northern Greece also show negative values or values close to zero. On the contrary, stations in central Greece, where the network was very sparse show very low sensitivity ($\mu > 0$) during the period 1963–2000. Their sensitivity increased slightly
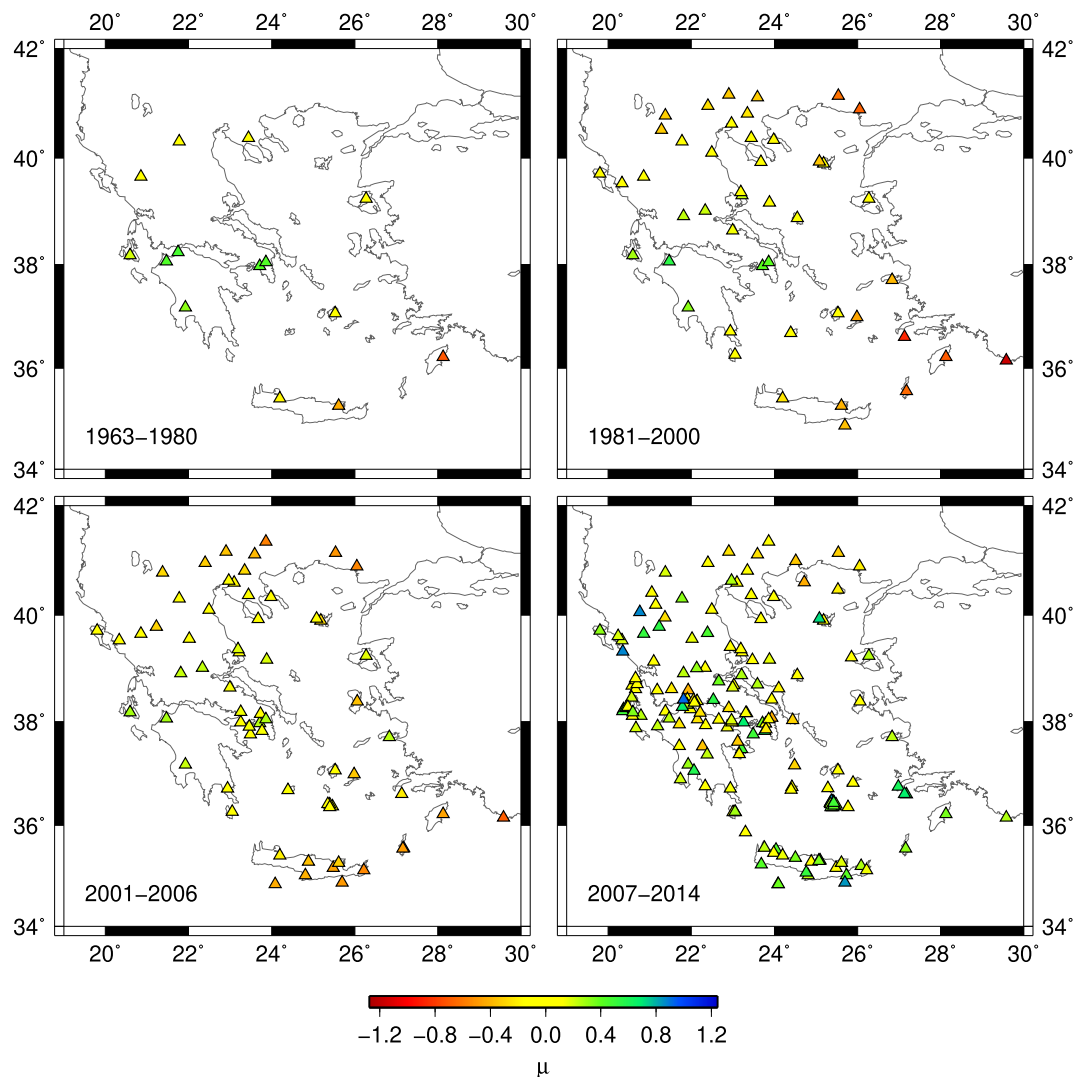
Figure 8. Maps showing the sensitivity (μ) of the seismic stations operating in Greece for four different periods as determined by applying the method summarized in Fig. 6.

during the third period (2001–2006), when some of them operated as digital stations. During the last period (2007–2014), one would expect that the majority of the stations would show higher sensitivity. However, the opposite is observed which indicates that the analysis must have been predominantly focused on picking seismic phases in local distance. This is also evident from diagrams similar to Fig. 6 for the rest of the seismic stations. This indicates that the majority of the stations are able to detect seismic events of $M_L \sim 3.5$ even in long distances (up to 800 km, see results for the 2001–2006 time period). In contrast, during the most modern period (2007–2014), this ability is not evident. This most likely happens due to the fact that the analysts avoid systematic phase picking from long distance stations, and focus their analysis only to the stations within the local epicentral distances (up to 100 km), in order to cope with their workload as consequence of the large number of operating stations. This pattern is common in the majority of the analysed stations in this study. The fact that the detection threshold of the network for the last period appears significantly low compared to the earlier periods (see Fig. 7), has to do primarily with the very good coverage of the network as a whole from 2007 to 2014 with overall low interstation distance.

4.2 Magnitude of completeness assessment of the NOA network using the PMC method

We first determined the on-/off-times of each station directly from the phase-arrival data (see also Fig. S3, Supporting Information) that we used in Section 4.1, and we calculated detection probabilities $P_D(M, L)$ for each station. We used a magnitude interval of 0.1 magnitude units and a distance interval of 0.1° and we compiled completeness magnitude (M_P) maps for a 15 km depth layer (see Animation S1 in the Supporting Information). Fig. 9 shows the most significant changes in the performance of the network over time, at 15 km depth, based on the completeness magnitude analysis using the PMC method. We selected to use this depth value as the majority of the seismicity in our data set is shallow (< 30 km). It is evident that the performance of the network remained relatively poor until 1990. It is worth mentioning that even when the THE network came into operation in 1981, it only contributed significantly since 1990, focusing on analysing the local seismicity in northern Greece. Additional stations installed and operated in central Greece since 2004 extended the area of the minimum completeness magnitude towards southern Greece, but it was only until 2010 when the network operated in a satisfactory degree offering the capability to
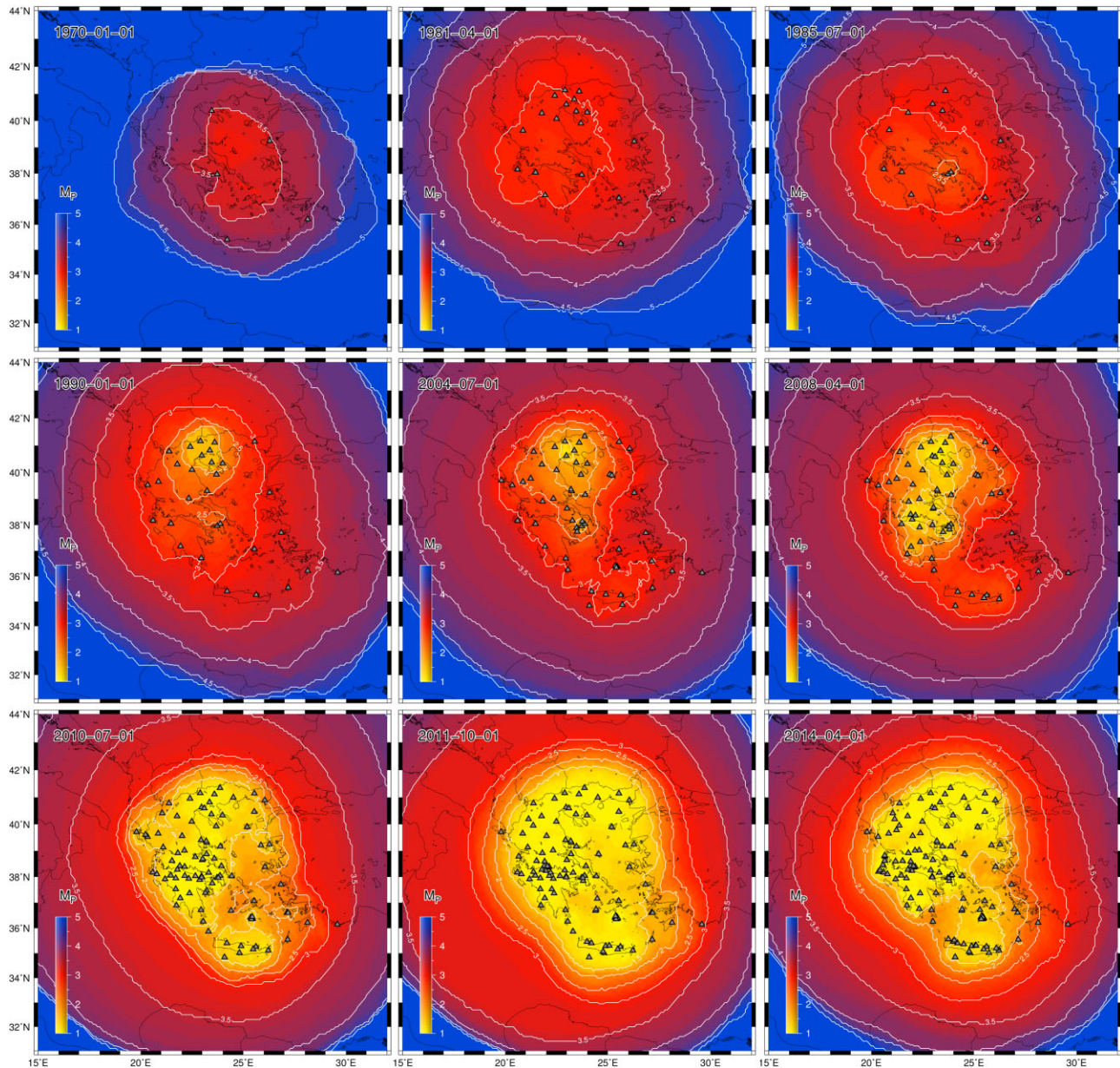
Figure 9. Maps showing the spatial distribution of the completeness magnitude (M_P) at 15 km depth, based on the stations (grey triangles) operated in Greece at different times. Maps are generated in three-month intervals but only a subset of them is shown here.

detect earthquakes of small magnitudes (∼1) within the whole area of its station coverage.

In addition, we compiled event-probability maps ($P_E(M, \mathbf{x})$, see Animations S2–S5 in the Supporting Information) for a 15 km depth layer and four different magnitudes (1.0, 1.5, 2.5 and 3.5). Fig. 10 shows an example for the depth of 15 km with data obtained from the three-month time windows starting in July 1994, 2004 and 2014, respectively. The detection of very small-magnitude events (∼1.0) by the Unified Network is only possible within the last few years (since approximate 2010) based on our analysis. Even so, this is limited to earthquakes that occur in mainland Greece only, where the network coverage is very good. Slightly larger magnitude earthquakes (∼1.5) used to be detected from the THE network in northern Greece since the mid-1990s, and it was only over the last years of operation of the Unified Network that these seismic events were detected in the entire area of Greece. The only exception is the south-east part (Rhodes

and Kastellorizo islands). For seismic events of magnitude 2.5, the detection capability of the network was limited in mainland Greece until mid-2000s, whereas the performance of the network improved over the last decade. Finally, seismic events of magnitude 3.5 were detected to a satisfactory degree over the entire period examined in this section, with a clear improvement towards the most recent years.

5 DISCUSSION

We presented a complete assessment of detection capabilities of the seismic stations in Greece and the completeness magnitude for the seismic network of Greece during the period from 1964 to 2014. The analysis was based not only on the available seismic catalogues, but more importantly we extracted spatio-temporal data
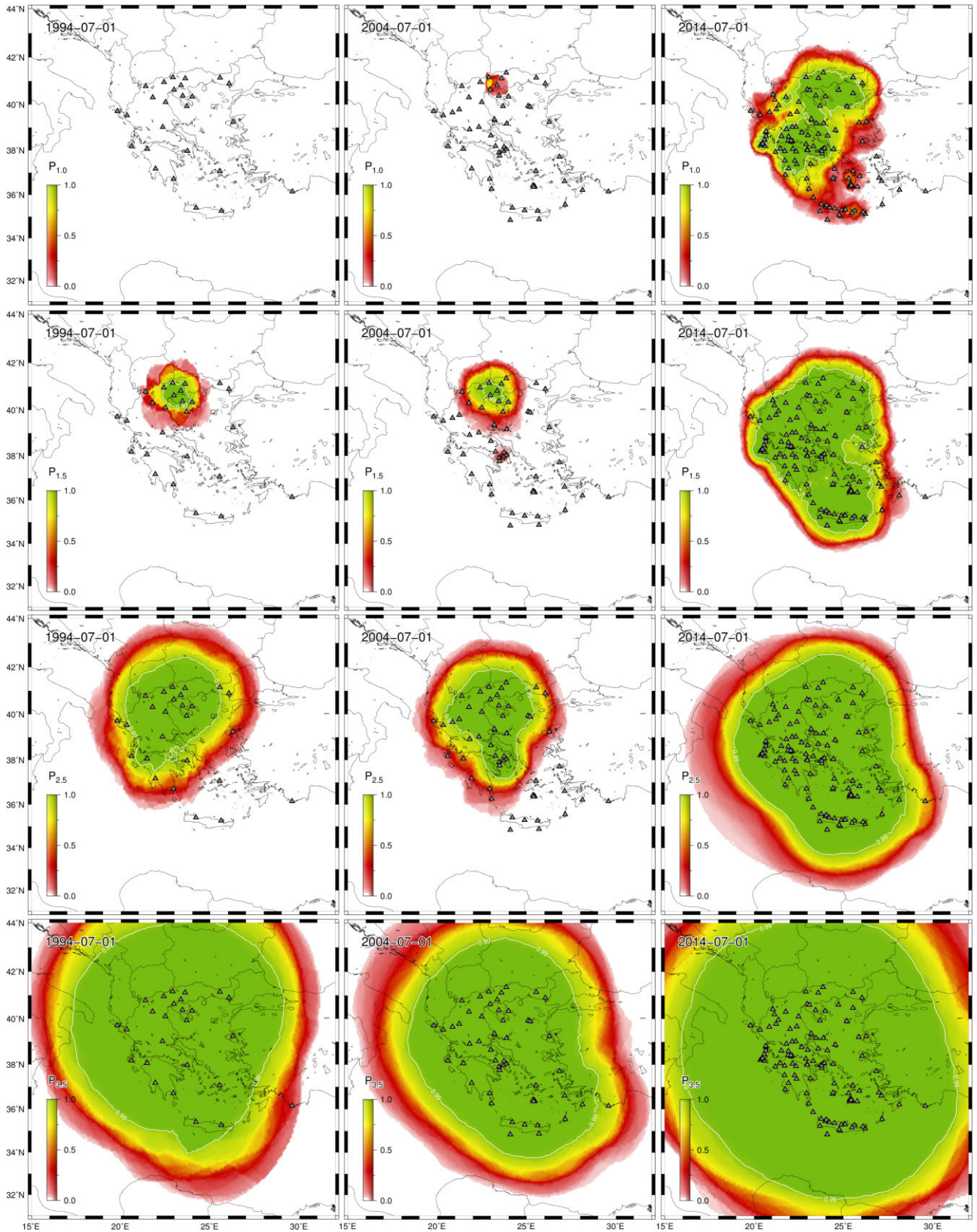
Figure 10. Event-detection probability (P_E) maps at 15 km at different times, covering three decades of operation, and for magnitudes of 1.0, 1.5, 2.5 and 3.5. Maps are generated in three-month intervals but only a subset of them is shown here. Seismic stations are shown as grey triangles.

by using the manually picked phase arrivals which are associated with the hypocentre solutions in the catalogues. Specifically, we used data from ISC which combines the two existing seismic catalogues, reported by NOA and THE, and are merged into a single catalogue that represents the most complete source of seismicity in Greece based on observations from permanent stations.

We applied two different methods, namely, we calculated station detection capability thresholds based on a technique that was applied to the stations of the International Monitoring System (IMS) by Kvaerna & Ringdal (2013), and the PMC technique developed by Schorlemmer & Woessner (2008). The first method is simple and does not require any additional information, such as signal-to-noise ratio (SNR) for the detected phases, or noise levels for the non-detected phases. Nonetheless, attractive by its simplicity, this method is not very stable for regions with limited numbers of seismic events, and its efficiency is a function of the grid size. In our case, we used a fine grid of $0.2° \times 0.2°$ which provided a good balance between resolution and efficiency. The second method is a much more advanced technique that calculates the completeness magnitude and the probability of detecting a seismic event for a given magnitude and location, by taking into account phase arrivals and extracting spatio-temporal characteristics of the network from the data. This method was applied in several other cases (Nanjo *et al.* 2010; Schorlemmer *et al.* 2010b; Gentili *et al.* 2011; Plenkers *et al.* 2011; Schorlemmer *et al.* 2018) and it can provide the basis for quantitative evaluation of forecasting models (Schorlemmer et al. 2010a), and/or it can highlight areas of poor detection capabilities for further improvement.

Comparing the detection thresholds and completeness magnitude distributions from both techniques (see e.g. Figs 7 and 9), we found that even though they follow different approaches, their results are comparable overall, which is encouraging. For example, the application of both methods was on the basis of different time windows, with the method of calculating station detection thresholds being applied in four major periods as explained in Section 4.1, whilst the completeness magnitude was calculated in three-month time windows (see Animation S1 in the Supporting Information). Nevertheless, both techniques agree that the major improvement of the performance of the network as a whole occurred approximately in 2008, whereas prior to this (2000–2007) the best-performing area was northern Greece as a consequence of the operation of the regional network of THE. During the early period (up to 1985), the overall detection capabilities in Greece were rather poor as it was shown by both techniques. It is worth noting that apart from the fundamental differences between the two techniques, station detection-capability thresholds calculated by the method based on Kvaerna & Ringdal (2013) are underestimated by approximately 0.5 in magnitude in comparison to PMC. We believe that this is probably due to the fact that longer periods are being used in the method based on Kvaerna & Ringdal (2013) and the results are an average representation of the overall performance of the network for each period.

Furthermore, comparing the results in this paper, especially the completeness magnitude distributions obtained with the PMC method with results of previous studies, we found that Mignan & Chouliaras (2014) have overestimated the capabilities of the network in central Greece up to 2008, even though they applied a Bayesian magnitude of completeness (BMC) method (Mignan *et al.* 2011) that takes into account the spatial characteristics of the data. This is probably a result of not taking into consideration data from the THE network that operated separately at this period, hence, their catalogue could be considered somewhat incomplete in northern Greece (Marzocchi *et al.* 2003). From 2008 onwards, when the unified network (HUSN) was in operation, their results are similar to those obtained in the current study. D'Alessandro *et al.* (2011) on the other hand, studied the hypocentral location capabilities of the unified network (HUSN) for the period from

2007 to June 2010. Specifically, they determined the uncertainties in hypocentre locations from evaluating the background-noise levels recorded at the stations of the network and they computed the completeness magnitude of the network for seismic events that trigger at least four stations. They mention that their completeness magnitude is overestimated as they do not take into account the spatial characteristics of the network and the hypocentral distances or the errors of the velocity model used in their locations. Indeed, comparing the results of the current study for the period covered by D'Alessandro *et al.* (2011), we found that their results agree better with ours only for 2010, whereas for the period prior to this, our estimations on the completeness magnitude are more conservative.

6 CONCLUSIONS

In this paper, we assessed the network sensitivity in Greece over a long period range in the most realistic way to our knowledge. For this reason, we avoided the use of Gutenberg–Richter based methods that only use seismic catalogues as their input, and ignore the periods of low-detection capability (Wiemer & Wyss 2000). In contrast, we used manually picked phase arrivals, after combining all the available seismic catalogues based on observations from permanent stations in the area and we applied two different techniques with different levels of complexity which yielded comparable results. Notably, we observed a substantial improvement in earthquake detection capabilities for North Greece that took place around 1990 as a result of the operation of the regional network of the THE, and an overall drop in the completeness magnitude ($M_p \sim 1$) throughout Greece after the establishment and operation of the unified network (HUSN) from 2008 onwards.

DATA AVAILABILITY

The data underlying this paper are available in the ISC website (http://www.isc.ac.uk/iscbulletin/search/), at https://doi.org/10.31905/D808B830.

SUPPORTING INFORMATION

Supplementary data are available at *GJI* online.

suppl_data

Please note: Oxford University Press is not responsible for the content or functionality of any supporting materials supplied by the authors. Any queries (other than missing material) should be directed to the corresponding author for the paper.

REFERENCES

Ambraseys, N.N. & Jackson, J.A., 1990. Seismicity and associated strain of Central Greece between 1890 and 1988, *Geophys. J. Int.,* **101**(3), 663–708.

Baskoutas, I.G., Kalogeras, I.S., Kourouzidis, M. & Panopoulou, G., 2000. a modern technique for the retrieval and processing of historical seismograms in Greece, *Nat. Hazards,* **21**(1), 55–64.

Bondár, I. & Storchak, D.A., 2011. Improved location procedures at the International Seismological Centre, *Geophys. J. Int.,* **186**(3), 1220–1244.

Burton, P.W., Xu, Y., Qin, C., Tselentis, G.-A. & Sokos, E., 2004. A catalogue of seismicity in Greece and the adjacent areas for the twentieth century, *Tectonophysics,* **390**(1), 117–127.

Comninakis, P.E. & Papazachos, B.C., 1972. Seismicity of the Eastern Mediterranean and some tectonic features of the Mediterranean Ridge, *Bull. geol. Soc. Am.,* **83**(4), 1093.

D'Alessandro, A., Papanastassiou, D. & Baskoutas, I., 2011. Hellenic Unified Seismological Network: an evaluation of its performance through SNES method, *Geophys. J. Int.,* **185**(3), 1417–1430.

DiGiacomo, D., Engdahl, E.R. & Storchak, D.A., 2018. The ISC-GEM Earthquake Catalogue (1904–2014): status after the extension project, *Earth Syst. Sci. Data,* **10**(4), 1877–1899.

Eginitis, D., 1932. *Annales De L' Observatoire National D' Athènes,* Vol. **12**, Imprimerie Royale Ingelsi-Papageorgiou.

Evangelidis, C.P. *et al.*, 2021. Seismic waveform data from Greece and Cyprus: integration, archival, and open access, *Seismol. Res. Lett.,* **92**(3), 1672–1684.

Gentili, S., Sugan, M., Peruzza, L. & Schorlemmer, D., 2011. Probabilistic completeness assessment of the past 30 years of seismic monitoring in Northeastern Italy, *Phys. Earth planet. Inter.,* **186**(1–2), 81–96.

Hunter, J.D., 2007. Matplotlib: a 2D graphics environment, *Comput. Sci. Eng.,* **9**(3), 90–95.

Hutton, L.K. & Boore, D.M., 1987. The ML scale in Southern California, *Bull. seism. Soc. Am.,* **77**(6), 2074–2094.

International Seismological Centre, 2013. *Summary of the Bulletin of the International Seismological Centre,* January To June 2010, Vol. 47, Issue 1–6, Zenodo. https://doi.org/10.5281/zenodo.998584.

International Seismological Centre, 2022. *On-line Bulletin,* http://www.isc.ac.uk.

ISS, 1938–1963. *International Seismological Summary, Annual Volumes.*

Jackson, J., Gagnepain, J., Houseman, G., King, G., Papadimitriou, P., Soufleris, C. & Virieux, J., 1982. Seismicity, normal faulting, and the geomorphological development of the Gulf of Corinth (Greece): The Corinth Earthquakes of February and March 1981, *Earth planet. Sci. Lett.,* **57**(2), 377–397.

Kiratzi, A. & Papazachos, B., 1984. Magnitude scales for earthquakes in Greece, *Bull. seism. Soc. Am.,* **74**. https://doi.org/10.1785/BSSA0740030969.

Koutsoukos, E. & Melis, N., 2005. A horizontal component broadband seismic sensor based on an inverted pendulum, *Bull. seism. Soc. Am.,* **95**, 2462–2471.

Koutsoukos, E.T. & Melis, N.S., 2007. Broadening the response of short-period sensors: an application to the Sprengnether S-7000 seismometer, *Bull. seism. Soc. Am.,* **97**(4), 1212–1220.

Kuyuk, H.S. & Allen, R.M., 2013. Optimal seismic network density for earthquake early warning: a case study from California, *Seismol. Res. Lett.,* **84**(6), 946–954.

Kvaerna, T. & Ringdal, F., 2013. Detection capability of the seismic network of the international monitoring system for the comprehensive nuclear-test-ban treaty, *Bull. seism. Soc. Am.,* **103**(2A), 759–772.

Landro, G.D., Picozzi, M., Russo, G., Adinolfi, G.M. & Zollo, A., 2019. Seismic networks layout optimization for a high-resolution monitoring of induced micro-seismicity, *J. Seismol.,* **24**(5), 953–966.

Lentas, K. & Harris, J., 2019. Enhanced performance of ISC focal mechanism computations as a result of automatic first-motion polarity picking optimization, *J. Seismol.,* **23**, 1141–1159.

Leptokaropoulos, K.M., Papadimitriou, E.E., Orlecka-Sikora, B. & Karakostas, V.G., 2012. Seismicity rate changes in association with the evolution of the stress field in Northern Aegean Sea, Greece, *Geophys. J. Int.,* **188**(3), 1322–1338.

Li, B., Sørensen, M.B., Atakan, K., Li, Y. & Li, Z., 2020. Probabilistic seismic hazard assessment for the shanxi rift system, North China, *Bull. seism. Soc. Am.,* **110**(1), 127–153.

Lombardi, A.M., Cocco, M. & Marzocchi, W., 2010. On the increase of background seismicity rate during the 1997-1998 Umbria-Marche, Central Italy, sequence: apparent variation or fluid-driven triggering?, *Bull. seism. Soc. Am.,* **100**(3), 1138–1152.

Makropoulos, K., Kaviris, G. & Kouskouna, V., 2012. An updated and extended earthquake catalogue for Greece and adjacent areas since 1900, *Nat. Hazards Earth Syst. Sci.,* **12**(5), 1425–1430.

Makropoulos, K.C., Drakopoulos, J.K. & Latousakis, J.B., 1989. A revised and extended earthquake catalogue for Greece since 1900, *Geophys. J. Int.,* **98**(2), 391–394.

Marzocchi, W., Sandri, L. & Boschi, E., 2003. On the validation of earthquake-forecasting models: the case of pattern recognition algorithms, *Bull. seism. Soc. Am.,* **93**(5), 1994–2004.

Melis, N.S. & Konstantinou, K.I., 2006. Real-time seismic monitoring in the Greek Region: an example from the 17 October 2005 East Aegean Sea earthquake sequence, *Seismol. Res. Lett.,* **77**(3), 364–370.

Melis, N.S., Brooks, M. & Pearce, R.G., 1989. A microearthquake study in the Gulf of Patras Region, Western Greece, and its seismotectonic interpretation, *Geophys. J. Int.,* **98**(3), 515–524.

Mignan, A. & Chouliaras, G., 2014. Fifty Years of seismic network performance in Greece (1964-2013): spatiotemporal evolution of the completeness magnitude, *Seismol. Res. Lett.,* **85**(3), 657–667.

Mignan, A., Werner, M.J., Wiemer, S., Chen, C.-C. & Wu, Y.-M., 2011. Bayesian estimation of the spatially varying completeness magnitude of earthquake catalogs, *Bull. seism. Soc. Am.,* **101**(3), 1371–1385.

Morandi, M.T. & Matsumura, S., 1991. Update on the examination of the seismic observational network of the National Research Institute for Earth Science and Disaster Prevention (NIED)—detection capability and magnitude correction, **47**.

Nanjo, K.Z., Schorlemmer, D., Woessner, J., Wiemer, S. & Giardini, D., 2010. Earthquake detection capability of the Swiss Seismic Network, *Geophys. J. Int* https://doi.org/10.1111/j.1365-246X.2010.04593.x.

Nyst, M. & Thatcher, W., 2004. New constraints on the active tectonic deformation of the aegean, *J. geophys. Res.: Solid Earth,* **109**(B11). https://doi.org/10.1029/2003JB002830.

Oliver, J. & Murphy, L., 1971. WWNSS: seismology's Global Network of Observing Stations, *Science,* **174**(4006), 254–261.

Papazachos, B., 1990. Seismicity of the aegean and surrounding area, *Tectonophysics,* **178**(2–4), 287–308.

Papazachos, B. & Comninakis, P., 1978. Deep structure and tectonics of the Eastern Mediterranean, *Tectonophysics,* **46,** 285–296.

Papazachos, B., Mountrakis, D., Psilovikos, A. & Leventakis, G., 1979. Surface fault traces and fault plane solutions of the May–June 1978 major shocks in the Thessaloniki area, Greece., *Tectonophysics,* **53**(3–4), 171–183.

Papazachos, B., Comninakis, P., Mountrakis, D. & Pavlides, S., 1982. Preliminary results of an investigation of the February-March Alkionides Gulf (Greece) earthquakes, *Proc. Int. Symp. Hellenic Arc Trench,* **2,** 74–87.

Papazachos, V. & Papazachou, C., 1997. *The Earthquakes of Greece, Editions Ziti*. Editions Ziti.

Peterson, J.R. & Hutt, C.R., 2014. *World-Wide Standardized Seismograph Network: A Data Users Guide: U.S. Geological Survey Open-File Report 2014–1218,* 74, https://dx.doi.org/10.3133/ofr20141218. ISSN 2331-1258 (online).

Plenkers, K., Schorlemmer, D. & Kwiatek, G., 2011. On the probability of detecting picoseismicity, *Bull. seism. Soc. Am.,* **101**(6), 2579–2591.

Richter, C.F., 1935. An instrumental earthquake magnitude scale, *Bull. seism. Soc. Am.,* **25**(1), 1–32.

Ringdal, F., 1975. On the estimation of seismic detection thresholds, *Bull. seism. Soc. Am.,* **65**(6), 1631–1642.

Saltogianni, V., Mouslopoulou, V., Oncken, O., Nicol, A., Gianniou, M. & Mertikas, S., 2020. Elastic fault interactions and earthquake rupture along the Southern Hellenic subduction plate interface zone in Greece, *Geophys. Res. Lett.,* **47**(13). https://doi.org/10.1029/2019GL086604.

Schorlemmer, D. & Woessner, J., 2008. Probability of detecting an earthquake, *Bull. seism. Soc. Am.,* **98**(5), 2103–2117.

Schorlemmer, D., Christophersen, A., Rovida, A., Mele, F., Stucchi, M. & Marzocchi, W., 2010a. Setting up an earthquake forecast experiment in Italy, *Ann. Geophys.,* **53**(3). https://doi.org/10.4401/ag-4844.

Schorlemmer, D., Mele, F. & Marzocchi, W., 2010b. A completeness analysis of the national seismic network of Italy, *J. geophys. Res.,* **115**(B4). https://doi.org/10.1029/2008JB006097.

Schorlemmer, D., Hirata, N., Ishigaki, Y., Doi, K., Nanjo, K.Z., Tsuruoka, H., Beutin, T. & Euchner, F., 2018. *Earthquake Detection Probabilities in Japan.* Bulletin of the Seismological Society of America, **108**(2): 702–717. https://doi.org/10.1785/0120170110.

Toda, S., 2002. Response of the San Andreas Fault to the 1983 Coalinga-Nuñez Earthquakes: an application of interaction-based probabilities for Parkfield, *J. geophys. Res.,* **107**(B6). https://doi.org/10.1029/2001JB000172.

Wessel, P., Smith, W.H.F., Scharroo, R., Luis, J. & Wobbe, F., 2013. Generic Mapping Tools: improved version released, *Eos, Trans. Am. geophys. Un.,* **94**(45), 409–410.

Wiemer, S. & Wyss, M., 2000. Minimum magnitude of completeness in earthquake catalogs: examples from Alaska, the Western United States, and Japan, *Bull. seism. Soc. Am.,* **90**, 859–869.

Woessner, J. & Wiemer, S., 2005. Assessing the quality of earthquake catalogues: estimating the magnitude of completeness and its uncertainty, *Bull. seism. Soc. Am.,* **95**(2), 684–698.

Wood, H.O., 1921. *A List of Seismologic Station of the World, Bulletin of the National Research Council,* Vol. **2**, Part 7, Number 15. The National Research Council of The National Academy of Sciences, Washington, DC., USA.

Yamada, R., Garcia, R.F., Lognonné, P., Feuvre, M.L., Calvet, M. & Gagnepain-Beyneix, J., 2011. Optimisation of seismic network design: application to a geophysical International Lunar Network, *Planet. Space Sci.,* **59**(4), 343–354.

APPENDIX A: SEISMICITY MONITORING, INSTRUMENTATION, CATALOGUES AND BULLETINS IN GREECE

Seismicity in Greece has been monitored since ancient times, through historical macroseismic observations and damage description especially for catastrophic earthquakes (Papazachos & Papazachou 1997). In 1893, the first attempts towards systematic seismological instrumental observations were based on the use of two Brassart seismoscopes in Athens. Other macroseismic observations were provided and systematically reported in the NOA Bulletin, by the assigned staff of local meteorological stations in several cities and towns around Greece.

The first attempt to instrumentally monitor the seismicity in Greece was initiated by NOA in 1899, and by 1903 a five-station network was deployed in Central Greece and the Peloponnese (Athens—June 1899, Chalkis—June 1900, Kalamata—September 1900, Zante—October 1902 and Aigion—January 1903). More details can be found in Wood (1921) and the NOA Bulletins. The NOA director at that time, Prof. D. Aiginitis, strongly supported the systematic observations of geodynamic phenomena and pushed for the installation. This basic network was equipped with Agamennone seismographs (two horizontal components) which at the time lacked damping. These instruments proved to be rather unreliable in operation and the network stayed in service only for a short period of time. Specifically, the Agamennone seismograph in Athens station operated until 1920, whereas the rest of the stations of the first network were dismissed before 1912 (Wood 1921) providing only small number of phase reporting as seen in the NOA Bulletins.

In 1911, the first upgrade at Athens station took place with the installation of a two horizontal components Mainka seismograph,

amongst the few operating stations in the East Mediterranean at that time, that provided usable readings for hundreds of earthquakes in the early part of the last century. Several other instruments were installed afterwards, in particular a two-component horizontal Wiechert seismograph was donated by Greek expats living in Germany in 1924. In 1928, a vertical component Wiechert seismograph was bought and installed in Athens, whereas in 1932, a horizontal component N-S, small gain seismograph designed and built by the Director of the Institute of Geodynamics, NOA at that time (Prof. N. Critikos) had also become operational (Wood 1921; Eginitis 1932). In September 1957, a Canada donation due to a visit of Prof. A. Galanopoulos Director of Institute of Geodynamics, NOA at that time, a vertical component, high gain amplification Benioff seismograph was also installed in Athens at the same vault facilities (Baskoutas et al. 2000).

In 1962, the ATH station vault at NOA was extended to its existing form, in the basement of the Institute of Geodynamics (main building at Thissio, Athens), in order to host three short-period Benioff type seismometers (three-component station) operated at period 1 s and three long-period Sprengnether Press–Ewing type seismometers (three-component station) operated at period 15 s, according to the standards of the World-Wide Standardized Seismograph Network (WWSSN, Oliver & Murphy 1971). The installation was done according to WWSSN standards (Peterson & Hutt 2014). Magnification and other operating information can be found in the NOA Bulletins, published every year at that time. Moreover, a vertical-component Wiechert with 80 kg pendulum mass, Spindler and Hoer manufactured seismograph was installed in Patras in 1963, and a three-component, Hiller seismograph was put into service in Athens (Athens vault) in July 1964.

In 1964 efforts began to develop an analogue National Seismic Network to cover the entire country following global standards of that period and record on photographic paper. Vaults were designed following WWSSN standards. Over 10 yr time 10 new stations (out of the 14 originally planned) were installed. In 1965, a Wood–Anderson seismograph (two horizontal components) was installed in Athens in order to provide proper amplitude measurements for local earthquake magnitude M_L (Richter 1935) calculations. During autumn 1965, four additional three-component stations (PRK: Agia Paraskevi—Lesvos, VLS: Valsamata—Cephalonia, ARG: Archangellos—Rhodes and VAM: Vamos—Crete) were equipped with three short-period Sprengnether S-7000 seismometers (Koutsoukos & Melis 2007), one for each component. In 1968, two new stations were installed in Ioannina (JAN) NW Greece and Poligyros (PLG) in Chalkidiki, similarly equipped with three short-period Sprengnether S-7000 seismometers, and in 1971 Benioff (short-period vertical) and Hiller (three long-period) seismometers were transferred and installed in Penteli (PTL)—northern Athens suburbs. Another three short-period Sprengnether S-7000 seismometers were installed in July 1972 in Kozani (KZN), West Macedonia and another Wood–Anderson analogue seismograph was installed at Valsamata (VLS) Cephalonia station in October 1973 with operation until September 1988. In 1975, two stations started operating in Neapolis (NPS) Crete and in Ithomi (ITM) Messinia—SW Peloponissos. These two three-component stations had three short-period Kirnos CBK-M3 seismometers operated at 2 s period. The National Seismic Network deployment operation was finalized by 1976, with the establishment of station Apeiranthos (APE) in Naxos, Cyclades (November 1975) using the usual three short-period Sprengnether S-7000 seismometers and the station

Riolos (RLS) south of Patras (July 1976) using only a vertical short-period Teledyne Geotech S-13 seismometer and closing the Patras (PAT) station which was established in 1963. Station coordinates and operating information can be found at the International Registry (IR, http://www.isc.ac.uk/registries/) and at https://bbnet.gein.noa.gr/HL/real-time-plotting/noa-stations-list/hl-network-and-collaborative-stations-information.

Following the M_w=6.2, 1978 June 20, Thessaloniki, and the M_w=6.6, 1981 February 25, East Corinth Gulf earthquakes (i.e. Papazachos *et al.* 1979; Jackson *et al.* 1982), NOA replaced the three-component short-period magnetic suspension Sprengnether seismometers that were in operation at that time (Koutsoukos & Melis 2005) with the modern Teledyne Geotech S-13 short-period vertical seismometers using frequency-modulated transmission through dedicated telephone lines for real-time recording of seismic signals at NOA. Before that, film records were sent to NOA in Athens in order to be processed and analysed with some months delay. The existing network was also expanded with an eight-station network deployed in Northern Greece by the Seismological Laboratory of the Aristotle University of Thessaloniki (AUTH). This expansion established the Seismological Network of Thessaloniki (THE) in 1981. Meanwhile, additional telemetric stations were installed in other places in Greece by NOA and THE, equipped with S-13 Teledyne Geotech seismometers, as well as temporary networks and some other permanent stations were deployed by the universities of Athens and Patras.

The digital era in Greece started during the period from 1998 to 2000, and the newly established HUSN in 2007 achieved the full link of all broadband and short-period stations to the National Seismic Network, which is sharing data between NOA and the Universities (Thessaloniki, Athens, Patras) in real-time. This became the basis of adding stations from other operating networks (e.g. Technical Educational Institute of Crete Seismic Network) and the strong-motion networks operated by NOA and ITSAK (Institute of Engineering Seismology and Engineering, Thessaloniki) that started getting upgraded in 2008. Today, the Institute of Geodynamics, NOA coordinates HUSN within a close collaboration with all partner networks and provides waveform data to the community in open access through a dedicated European Integrated Data Archive (EIDA) node, http://eida.gein.noa.gr/ (Evangelidis *et al.* 2021).

Since the early years of instrumental observations at the ATH station, seismic phase measurements were reported in the NOA bulletin following the global bulletin standards, and also included in the International Seismological Summary (ISS 1938–1963). In the following years, and as new stations were put into service, phase picks and hypocentre solutions determined at NOA were also reported to the ISC (International Seismological Centre 2022). Several efforts to review the seismicity catalogues in Greece have been carried out over the past few decades (i.e. Comninakis & Papazachos 1972; Papazachos & Comninakis 1978; Papazachos *et al.* 1982; Burton *et al.* 2004; Makropoulos *et al.* 1989, 2012) and since the early 1980s two institutions, namely NOA and AUTH, compiled separate seismicity catalogues on a routine basis, based on own seismic networks, which were both made available to the ISC. Through the efforts of joining phase data, a more complete revised bulletin/catalogue is compiled at the ISC that contains all available phase data (and sometimes also phase data from portable temporary networks). These data are nowadays also part of the ISC-GEM catalogue (e.g. DiGiacomo *et al.* 2018).